

Experimental demonstration of associative memory with memristive neural networks

Yuriy V. Pershin^{a,*}, Massimiliano Di Ventra^b

^a Department of Physics and Astronomy and USC Nanocenter, University of South Carolina, Columbia, SC 29208, United States

^b Department of Physics, University of California, San Diego, La Jolla, California 92093-0319, United States

ARTICLE INFO

Article history:

Received 21 November 2009

Received in revised form 29 April 2010

Accepted 3 May 2010

Keywords:

Memory

Resistance

Neural network hardware

Neural networks

ABSTRACT

Synapses are essential elements for computation and information storage in both real and artificial neural systems. An artificial synapse needs to remember its past dynamical history, store a continuous set of states, and be “plastic” according to the pre-synaptic and post-synaptic neuronal activity. Here we show that all this can be accomplished by a memory–resistor (*memristor* for short). In particular, by using simple and inexpensive off-the-shelf components we have built a memristor emulator which realizes all required synaptic properties. Most importantly, we have demonstrated experimentally the formation of associative memory in a simple neural network consisting of three electronic neurons connected by two memristor–emulator synapses. This experimental demonstration opens up new possibilities in the understanding of neural processes using memory devices, an important step forward to reproduce complex learning, adaptive and spontaneous behavior with electronic neural networks.

© 2010 Elsevier Ltd. All rights reserved.

1. Introduction

When someone mentions the name of a known person we immediately recall her face and possibly many other traits. This is because we possess the so-called associative memory—the ability to correlate different memories to the same fact or event (Anderson, 1976). This fundamental property is not just limited to humans but it is shared by many species in the animal kingdom. Arguably the most famous example of this are experiments conducted on dogs by Pavlov (1927) whereby salivation of the dog’s mouth is first set by the sight of food. Then, if the sight of food is accompanied by a sound (e.g., the tone of a bell) over a certain period of time, the dog learns to associate the sound to the food, and salivation can be triggered by the sound alone, without the intervention of vision.

Since associative memory can be induced in animals and we, humans, use it extensively in our daily lives, the network of neurons in our brains must execute it very easily. It is then natural to think that such behavior can be reproduced in artificial neural networks as well—a first important step in obtaining functionalities that resemble those of the human brain. The idea is indeed not novel and models of neural networks have been suggested over the years that could theoretically perform such a

function (Cooper, 2000; Gurney, 1997; Hopfield, 1982; Munakata, 2008). However, their experimental realization, especially in the electronic domain, has remained somewhat difficult. The reason is that an electronic circuit that simulates a neural network capable of associative memory needs two important components: neurons and synapses, namely connections between neurons. Ideally, both components should be of nanoscale dimensions and consume/dissipate little energy so that a scale up of such a circuit to the number density of a typical human brain (consisting of about 10^{10} synapses/cm²) could be feasible. While one could envision an electronic version of the first component relatively easily, an electronic synapse is not so straightforward to make. The reason is that the latter needs to be flexible (“plastic”) according to the type of signal it receives, its strength has to depend on the dynamical history of the system, and it needs to store a continuous set of values (analog element).

In the past, several approaches with different levels of abstraction were used in order to implement electronic analogues of synapses (Lewis & Renaud, 2007). For instance, one of the first ideas involved the use of three-terminal electrochemical elements controlled by electroplating (Widrow, 1962). While some of these approaches do not involve synaptic plasticity at all (Jung, Brauer, & Abbas, 2001; Le Masson, Renaud-Le Masson, Debay, & Bal, 2002; Mahowald & Douglas, 1991; Sorensen, DeWeerth, Cymbalyuk, & Calabrese, 2004), the latter is generally implemented using digital (or a combination of analog and digital) hardware (Arthur & Boahen, 2006; Bofill, Murray, & Thompson, 2001; Glackin, McGinnity, Maguire, Wu, & Belatreche, 2005; Indiveri, Chicca,

* Corresponding author. Tel.: +1 803 777 5073; fax: +1 803 777 3065.

E-mail addresses: pershin@physics.sc.edu (Y.V. Pershin), diventra@physics.ucsd.edu (M. Di Ventra).

& Douglas, 2006; Linares-Barranco, Sanchez-Sinencio, Rodriguez-Vazquez, & Huertas, 1993; Schemmel, Meier, & Mueller, 2004; Vogelstein, Malik, & Cauwenberghs, 2007). The common feature of synaptic plasticity realizations is the involvement of many different circuit elements (such as transistors) and, therefore, occupation of a significant amount of space on a VLSI chip. Thus, the amount of electronic synapses in present VLSI implementations is much lower than the amount of synapses relevant to actual biological systems. Novel, radically different approaches to resolve this issue would be thus desirable.

A recently demonstrated resistor with memory (memristor for short Chua, 1971; Chua & Kang, 1976) based on TiO₂ thin films (Strukov, Snider, Stewart, & Williams, 2008; Yang et al., 2008) offers a promising realization of a synapse whose size can be smaller than 50 × 50 × 50 nm³. Using TiO₂ memristors, a fabrication of neuromorphic chips with a synapse density close to that of the human brain may become possible. Memristors belong to the larger class of memory-circuit elements (which includes also memcapacitors and meminductors) (Di Ventra, Pershin, & Chua, 2009), namely circuit elements whose response depends on the whole dynamical history of the system. Memristors can be realized in many ways, ranging from oxide thin films (Driscoll, Kim, Chae, Di Ventra, & Basov, 2009a; Driscoll et al., 2009b; Strukov et al., 2008; Yang et al., 2008) to spin memristive systems (Pershin & Di Ventra, 2009a; Pershin & Ventra, 2008). However, all these realizations are limited to the specific material or physical property responsible for memory, and as such they do not easily allow for tuning of the parameters necessary to implement the different functionalities of electronic neural networks.

In the present paper, we describe a flexible platform allowing for simulation of different types of memristors, and experimentally show that a memristor could indeed function as a synapse. We have developed electronic versions of neurons and synapses whose behavior can be easily tuned to the functions found in biological neural cells. Of equal importance, the electronic neurons and synapses were fabricated using inexpensive off-the-shelf electronic components resulting in few dollars cost for each element, and therefore can be realized in any electronic laboratory. Clearly, we do not expect that with such elements one can scale up the resulting electronic neural networks to the actual brain density. However, due to their simplicity reasonably complex neural networks can be constructed from the two elemental blocks developed here and we thus expect several functionalities could be realized and studied. We emphasize that all results reported in this paper are based on measurements of real electronic circuit response, without using SPICE modeling.

For the purpose of this paper we have built the neural network shown in Fig. 1. We have then shown that such circuit is capable of associative memory. In this network, two input neurons are connected with an output neuron by means of synapses. As an example of the functionality that this network can provide, we can think about the animal memory we have described above (Pavlov, 1927) in which the first input neuron (presumably located in the visual cortex) activates under a specific visual event, such as “sight of food”, and the second input neuron (presumably located in the auditory cortex) activates under an external auditory event, such as a particular “sound”. Depending on previous training, each of these events can trigger “salivation” (firing of the third (output) neuron). If, at a certain moment of time, only the “sight of food” leads to “salivation”, and subsequently the circuit is subjected to both input events, then, after a sufficient number of simultaneous input events the circuit starts associating the “sound” with the “sight of food”, and eventually begins to “salivate” upon the activation of the “sound” only. This process of learning is a realization of the famous Hebbian rule stating, in a simplified form, that “neurons that fire together, wire together”.

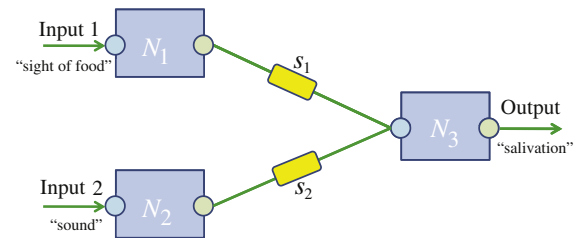


Fig. 1. Artificial neural network for associative memory. Real neurons and their networks are very complex systems whose behavior is not yet fully understood. However, some simple brain functions can be elucidated studying significantly simplified structures. Here, we consider three neurons (N_1 , N_2 and N_3) coupled by two memristive synapses (S_1 and S_2). The output signal is determined by input signals and strengths of synaptic connections which can be modified when learning takes place.

2. Results and discussion

2.1. Electronic neuron

Biological neurons deal with two types of electrical signals: receptor (or synaptic) potentials and action potentials. A stimulus to a receptor causes receptor potentials whose amplitude is determined by the stimulus strength. When a receptor potential exceeding a threshold value reaches a neuron, the latter starts emitting action potential pulses, whose amplitude is constant but their frequency depends on the stimulus strength. The action potentials are mainly generated along axons in the forward direction. However, there is also a back-propagating part of the signal (Stuart, Spruston, Sakmann, & Hausser, 1997; Waters, Schaefer, & Sakmann, 2005) which is now believed to be responsible for synaptic modifications (or learning) (Snider, 2008; Waters et al., 2005).

We have implemented the above behavior in our electronic scheme as shown in Fig. 2(a) using an analog-to-digital converter and a microcontroller. The input voltage is constantly monitored and once it exceeds a threshold voltage, both forward and backward pulses are generated whose amplitude is constant (we set it here for convenience at 2.5 V), but pulse separation varies according to the amplitude of the input signal. In Fig. 2(b) we show the response of the electronic neuron when three resistors of different values are subsequently connected between the input of the neuron and 2.5 V. When the resulting voltage (determined by the external resistor and internal resistor connected to the ground in Fig. 2(a)) is below the threshold voltage ($t < 1$ s in Fig. 2(b)), no “firing” occurs (no change in the output voltage). When the input voltage exceeds the threshold ($t > 1$ s in Fig. 2(b)), the electronic neuron sends forward- and back-propagating pulses. The pulse separation decreases with increase of the input voltage amplitude as it is evident in Fig. 2(b).

2.2. Electronic synapse

As electronic synapse we have built a *memristor emulator*, namely an electronic scheme which can simulate the behavior of almost any memory-resistor (Pershin & Di Ventra, in press, 2010). In fact, our memristor emulator can reproduce the behavior of any voltage- or current-controlled memristive system. The latter is described by the following relations

$$y(t) = g(x, y, t) u(t), \quad (1)$$

$$\dot{x} = f(x, u, t), \quad (2)$$

where $y(t)$ and $u(t)$ are input and output variables, such as voltage and current, $g(x, u, t)$ is a generalized response (memresistance R , or memductance G), x is a n -dimensional vector describing

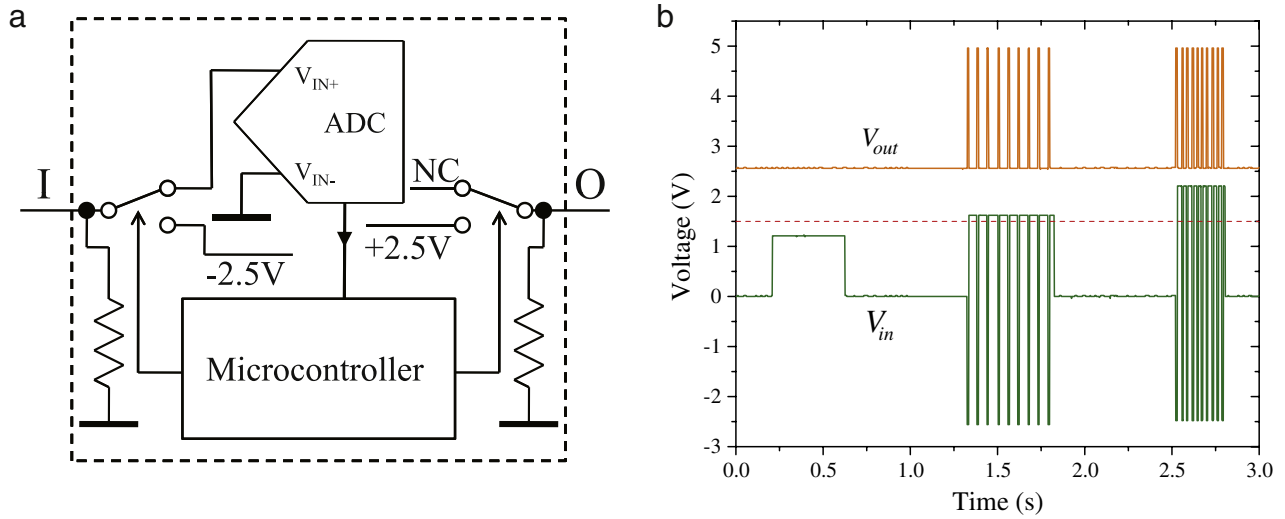


Fig. 2. Electronic neuron. **a**, Main components of the electronic neuron proposed here are an analog-to-digital converter (ADC) and a microcontroller. NC means not connected. If the voltage value V_{in} on the input terminal (I) exceeds a threshold voltage V_T (in our experiments $V_T = 1.5$ V), the microcontroller connects the input pin to -2.5 V and output pin (O) to 2.5 V for 10 ms, thus sending forward and backward pulses. After that, it waits for a certain amount of time δt and everything repeats again. If $V_{in} < V_T$, then the microcontroller just continuously samples V_{in} . The waiting time was selected as $\delta t = \tau - \gamma \cdot (V_{in} - V_T) + \lambda (\eta - 0.5)$, where $\tau = 60$ ms, $\gamma = 50$ ms/V, $\lambda = 10$ ms and η is a random number between 0 and 1. In our experimental realization, we used microcontroller dsPIC30F2011 from Microchip with internal 12 bits ADC and a possibility of pin multiplexing, so that the only additional elements were two 10 k resistors. Actual measurements were done using 5 V voltage span, with further assignment of the middle level as zero. The value of resistors shown in **a** is 10 k Ω . **b**, Response of the electronic neuron on input voltages of different magnitude, the red dashed line is the threshold voltage and is only a guide to the eye. When $V_{in} < V_T$, no firing occurs. When $V_{in} > V_T$, the electronic neuron sends pulses, with the average pulse separation decreasing with increasing V_{in} . V_{out} is shifted for clarity. (For interpretation of the references to colour in this figure legend, the reader is referred to the web version of this article.)

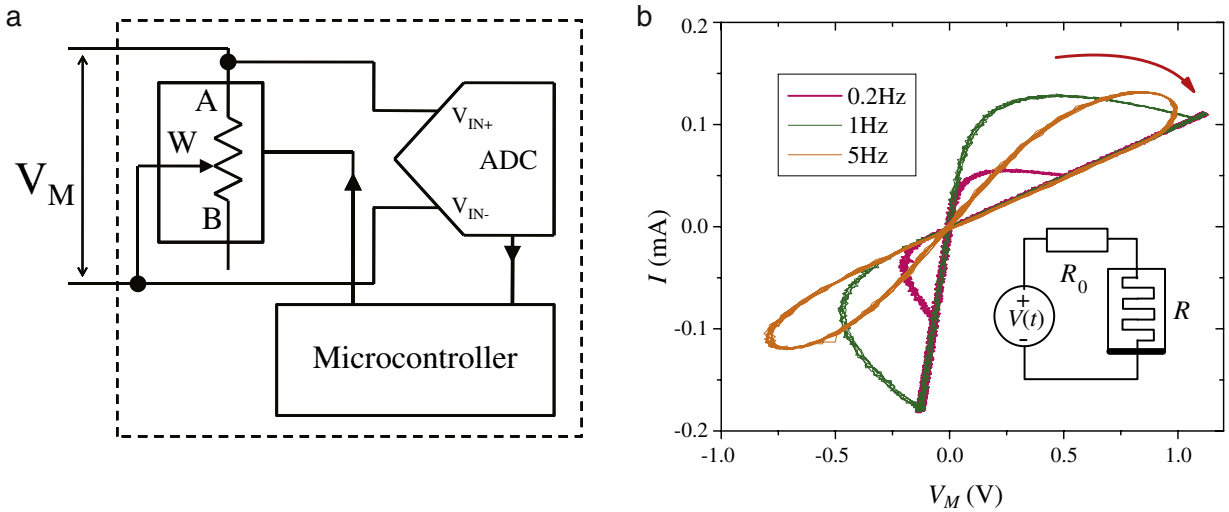


Fig. 3. Electronic synapse. **a**, Schematic of the main units of the memristor emulator. The memristor emulator consists of a digital potentiometer, ADC and microcontroller. The digital potentiometer unit represents an element whose resistance is defined by a digital code written in it. Two terminals of this unit (A and W) are the external connection terminals of the memristor emulator. The differential ADC converts the voltage between A and W terminals of the digital potentiometer into a digital value. The microcontroller reads the digital code from ADC and generates (and writes) a code for the digital potentiometer according to predefined functions $g(x, u, t)$ and $f(x, u, t)$ and Eqs. (1) and (2). These operations are performed continuously. In our circuit, we used a 256 positions 10 k Ω digital potentiometer AD5206 from Analog Device and microcontroller dsPIC30F2011 from Microchip with internal 12 bits ADC. **b**, Measurements of memristor emulator response when $V(t) = V_0 \cos(2\pi\omega t)$ with $V_0 \approx 2$ V amplitude is applied to the circuit shown in the inset with $R_0 = 10$ k Ω . The following parameters determining the memristor emulator response (see Eqs. (3) and (4)) were used: $\alpha = \beta = 146$ k Ω /(V s), $V_T = 4$ V, $R_1 = 675$ Ω , $R_2 = 10$ k Ω . We noticed that the initial value of R_M (in the present case equal to 10 k Ω) does not affect the long-time limit of the I - V curves. The signals were recorded using a custom data acquisition system.

the internal state of the device, and $f(x, u, t)$ is a continuous n -dimensional vector function (Chua & Kang, 1976; Di Ventra et al., 2009).

As Fig. 3(a) illustrates schematically, our memristor emulator consists of the following units: a digital potentiometer, an analog-to-digital converter and a microcontroller. The A (or B) terminal and the Wiper of the digital potentiometer serve as the external connections of the memristor emulator. The resistance of the digital potentiometer is determined by a code written into it by

the microcontroller. The code is executed by the microcontroller according to Eqs. (1) and (2). The analog-to-digital converter provides the value of voltage applied to the memristor emulator needed for the digital potentiometer code computation. The applied voltage can be later converted to the current since the microcontroller knows the value of the digital potentiometer resistance.

In our experiments, we implemented a threshold model of voltage-controlled memristor previously suggested in our earlier

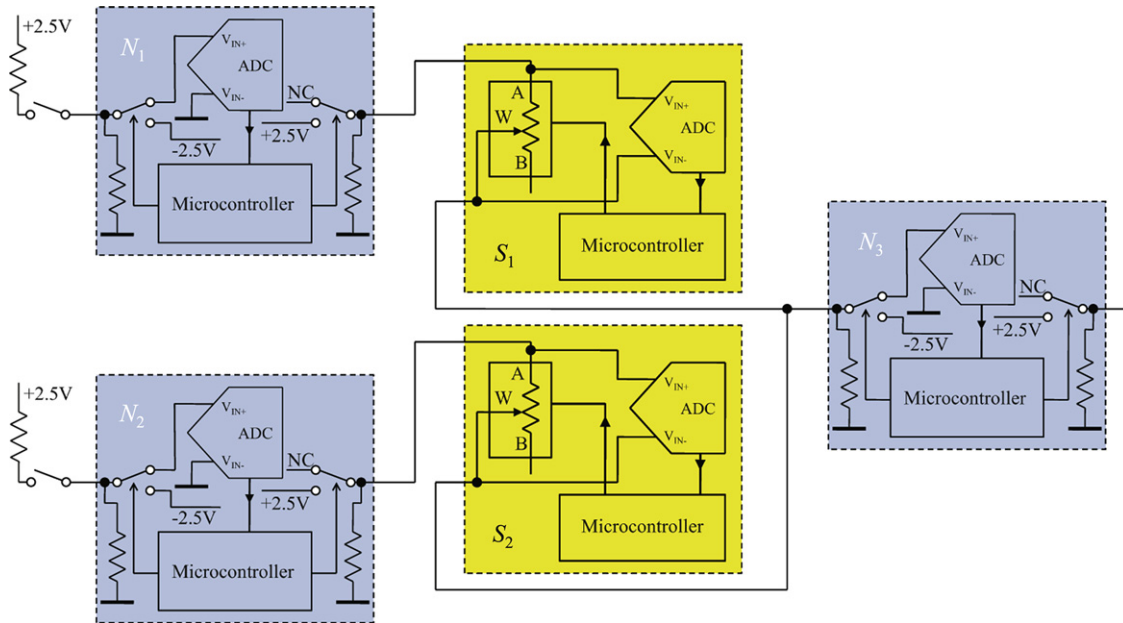


Fig. 4. Overall topology, at the component level, of our experimental realization of the neural network in Fig. 1. Two external switches connected to the inputs of N_1 and N_2 are used to apply input signals.

paper (Pershin, La Fontaine, & Di Ventra, 2009) and also discussed in (Di Ventra et al., 2009). In this model, the following equations (which are a particular case of Eqs. (1) and (2)) were used:

$$R = x, \quad (3)$$

$$\dot{x} = (\beta V_M + 0.5(\alpha - \beta)[|V_M + V_T| - |V_M - V_T|]) \times \theta(x - R_1) \theta(R_2 - x), \quad (4)$$

where $\theta(\cdot)$ is the step function, α and β characterize the rate of memristance change at $|V_M| \leq V_T$ and $|V_M| > V_T$, respectively, V_M is a voltage drop on memristor, V_T is a threshold voltage and R_1 and R_2 are limiting values of memristance. In Eq. (4), the θ -functions symbolically show that the memristance can change only between R_1 and R_2 . In the actual microcontroller's software implementation, the value of x is monitored at each time step and in the situations when $x < R_1$ or $x > R_2$, it is set equal to R_1 or R_2 , respectively. In this way, we avoid situations when x may overshoot the limiting values by some amount and thus not change any longer because of the step function in Eq. (4). In simple words, the memristance changes between R_1 and R_2 with different rates α and β below and above the threshold voltage. This activation-type model was inspired by recent experimental results on thin-film memristors (Yang et al., 2008) and as we discuss below it reproduces synapse plasticity.

To test that our emulator does indeed behave as a memristor, we have used the circuit shown in the inset of Fig. 3(b), in which an ac voltage is applied to the memristor emulator, R , connected in series with a resistor R_0 which was used to determine the current. The obtained current–voltage (I – V) curves, presented in Fig. 3(b), demonstrate typical features of memristive systems. For instance, all curves are pinched hysteresis loops passing through (0, 0) demonstrating no energy storage property of memristive systems (Chua & Kang, 1976; Di Ventra et al., 2009). Moreover, the frequency dependence of the curve is also typical for memristive systems: the hysteresis shrinks at low frequencies, when the system has enough time to adjust its state to varying voltage, and at higher frequencies, when the characteristic timescale of system variables change is longer than the period of voltage oscillations.

2.3. Associative memory

Using the electronic neurons and synapses described above, we have built an electronic scheme corresponding to the neural network depicted in Fig. 1. In this scheme (its circuit topology on the component level is shown in Fig. 4), we directly connect the memristor terminals to the input of the third (output) neuron N_3 . In such configuration, our network behaves essentially as a linear perceptron (Minsky & Papert, 1969; Rojas, 1996; Rosenblatt, 1958), although different connection schemes are possible. For example, putting a capacitor between the ground and the input of the third neuron N_3 , we would obtain an integrate-and-fire model (Gerstner & Kistler, 2002). In such a circuit (and also in perceptron networks with many synapses) it is important to ensure that the current from a synapse does not spread to its neighbors. This can be achieved by placing diodes between the right terminals of synapses in Fig. 1 and the input of the third neuron N_3 . For our neural network containing only two synapses the effect of current spreading between synapses is not important. Moreover, we would like to highlight that our neural network is fully asynchronous, in distinction to a scheme suggested by Snider (2008) based on a global clock. This makes our approach free of synchronization issues when scaling up and closer to a bio-inspired circuit. An asynchronous memristor-based network was also discussed recently (Linares-Barranco & Serrano-Gotarredona, 2009).

Fig. 5 demonstrates the associative memory development in the present network. Our experiment consists in application of stimulus signals to the first (“sight of food”) and second (“sound”) neurons, and monitoring of the output signal on the third (“salivation”) neuron. We start from a state when the first synaptic connection is strong (low resistance state of the first memristor) and second synaptic connection is weak (high resistance state of the second memristor).

In the first “probing phase” ($t < 9$ s, Fig. 5) we apply separate non-overlapping stimulus signals to the “sight of food” and “sound” neurons. This results in the “salivation” neuron firing when a stimulus signal is applied to the “sight of food” neuron, but not firing when a stimulus signal is applied to the “sound” neuron. Electronically, it occurs because pulses generated by the “sight of

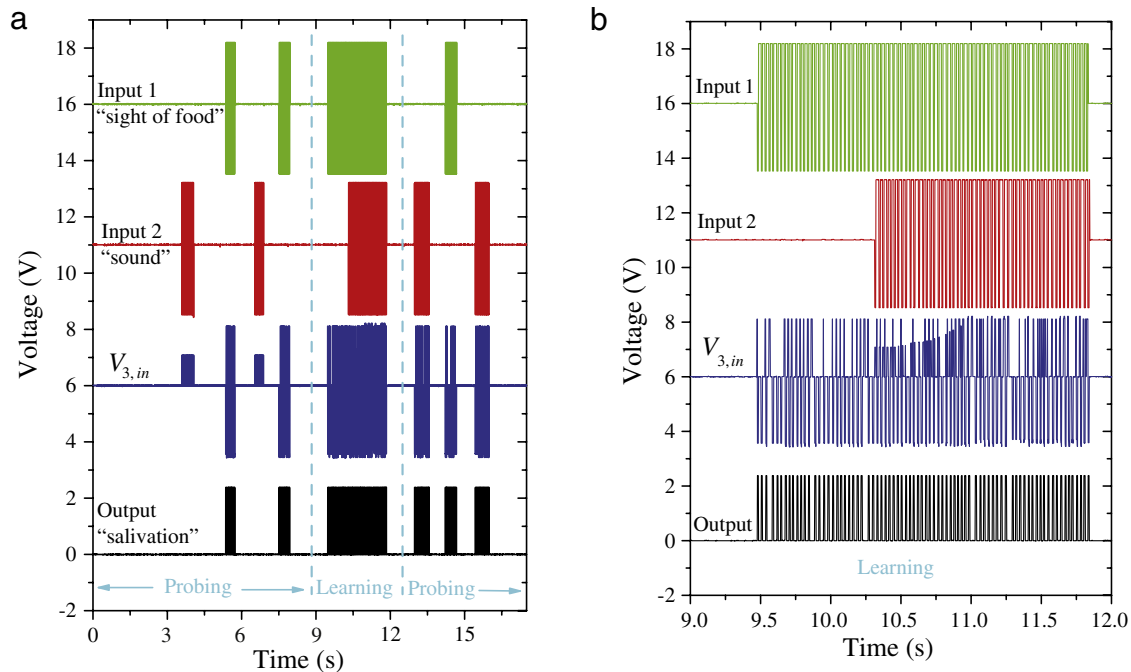


Fig. 5. Development of associative memory. **a**, Using electronic neurons and electronic synapses (memristor emulators), we have built an electronic circuit corresponding to the neural network shown in Fig. 4. We have used the following parameters defining the operation of memristor emulators: $V_T = 4$ V, $\alpha = 0$, $\beta = 15$ k Ω /(V s). At the initial moment of time, the resistance of S_1 was selected equal to $R_1 = 675$ Ω (lowest resistance state of memristor) and the resistance of S_2 was selected equal to $R_2 = 10$ k Ω (highest resistance state of memristor). Correspondingly, in the first probing phase, when Input 1 and Input 2 signals are applied without overlapping, the output signal develops only when Input 1 signal is applied. In the learning phase (see also **b** for more detailed picture), Input 1 and Input 2 signals are applied simultaneously. According to Hebbian rule, simultaneous firing of input neurons leads to development of a connection, which, in our case, is a transition of the second synapse S_2 from high- to low-resistance state. This transition is clearly seen as a growth of certain pulses in the signal $V_{3,in}$ (voltage at the input of third (output) neuron) in the time interval from 10.25 s to 11 s in **b**. In the subsequent probing phase, we observe that firing of any input neuron results in the firing of output neuron, and thus an associative memory realization has been achieved. The curves in **a** and **b** were displaced for clarity.

food” neuron exceed the threshold voltage of the “salivation” neuron (due to a low resistance of the first memristor synapse) while the voltage on the “salivation” neuron input due to the “sound” neuron pulses is below the threshold voltage of the “salivation” neuron. In this phase there is no memristor state change since the first memristor is already in its limiting state (with minimal resistance allowed) and its resistance cannot decrease further, and voltage drop on the second memristor is below its voltage threshold.

In the “learning phase” (9 s $< t < 12$ s, Fig. 5), stimulus voltages are applied simultaneously to both input neurons, thus generating trains of pulses. The pulses from different neurons are uncorrelated, but sometimes they do overlap, owing to a random component in the pulse separation (see Fig. 2 caption for details). During this phase, in some moments of time, back-propagating pulses from the “salivation” neuron (due to excitation from the “sight of food” neuron) overlap with forward propagating pulses from the “sound” neuron causing a high voltage across the second memristor synapse. As this voltage exceeds the memristor threshold, the second synapse state changes and it switches into a low resistance state. It is important to note that this change is possible when both stimuli are applied together (in other words they correlate). As a result, an association between input stimuli develops and the circuit “learns” to associate the “sight of food” signal to the “sound” signal.

Our measurements during the second probing phase ($t > 12$ s, Fig. 5) clearly demonstrate the developed association. It is obvious that, in this phase, any type of stimulus – whether from the “sight of food” or from the “sound” neurons – results in the “salivation” neuron firing.

Mention should be made about the memristor evolution function given by Eq. (4). In the present neural network the

resistance of the second synapse can only decrease, since only negative or zero voltages can be applied to the memristor. A process of synapse depression (corresponding to an increased synapse resistance in our electronic network) can be easily taken into account in different ways. The simplest way is to add a small positive constant to the first line of Eq. (4) (in the parentheses) for the conditioned memristor (S_2 in Fig. 1). Then, even at zero value of V_M , the resistance of the memristor will slowly increase. Another way is to apply a small positive bias to the conditioned memristor (S_2) in the circuit without any changes in Eq. (4) (this would also require taking a non-zero α).

3. Conclusion

We have shown that the electronic (memristive) synapses and neurons we have built can represent important functionalities of their biological counterparts, and when combined together in networks – specifically the one represented in Fig. 1 of this work – they give rise to an important function of the brain, namely associative memory. It is worth again mentioning that, although other memristors (e.g., those built from oxide thin films Borghetti et al., 2009) could replace the emulator we have built, the electronic neurons and synapses proposed here are electronic schemes that can be built from off-the-shelf inexpensive components. Together with their extreme flexibility in representing essentially any programmable set of operations, they are ideal to study much more complex neural networks (Likharev, Mayr, Muckra, & Turel, 2003) that could adapt to incoming signals and “take decisions” based on correlations between different memories. This opens up a whole new set of possibilities in reproducing different types of learning and possibly even more complex neural processes.

Acknowledgement

M.D. acknowledges the partial support from the National Science Foundation (DMR-0802830).

References

- Anderson, J. (1976). *Language, memory, and thought*. Hillsdale, NJ: Erlbaum.
- Arthur, J., & Boahen, K. (2006). In B. Sholkopf, & Y. Weiss (Eds.), *Advances in neural information processing systems: Vol. 18. Learning in silicon: timing is everything* (pp. 75–82). MIT Press.
- Bofill, A., Murray, A. F., & Thompson, D. P. (2001). In T. G. Dietterich, S. Becker, & Z. Ghahramani (Eds.), *Advances in neural information processing systems: Vol. 14. Circuits for VLSI implementation of temporally asymmetric Hebbian learning* (p. 1091). MIT Press.
- Borghetti, J., Li, Z., Straznicky, J., Li, X., Ohlberg, D. A. A., Wu, W., et al. (2009). A hybrid nanomemristor/transistor logic circuit capable of self-programming. *Proceedings of the National Academy of Sciences of the United States of America*, 106(6), 1699–1703.
- Chua, L. O. (1971). Memristor—the missing circuit element. *IEEE Transactions on Circuit Theory*, 18, 507–519.
- Chua, L. O., & Kang, S. M. (1976). Memristive devices and systems. *Proceedings of IEEE*, 64, 209–223.
- Cooper, L. (2000). Memories and memory: a physicist's approach to the brain. *International Journal of Modern Physics A*, 15(26), 4069–4082.
- Di Ventra, M., Pershin, Y. V., & Chua, L. O. (2009). Circuit elements with memory: memristors, memcapacitors, and meminductors. *Proceedings of IEEE*, 97(10), 1717–1724.
- Driscoll, T., Kim, H. T., Chae, B. G., Di Ventra, M., & Basov, D. N. (2009a). Phase-transition driven memristive system. *Applied Physics Letters*, 95, 043503.
- Driscoll, T., Kim, H.-T., Chae, B.-G., Kim, B.-J., Lee, Y.-W., Jokerst, N. M., et al. (2009b). Memory metamaterials. *Science*, 325, 1518–1521.
- Gerstner, W., & Kistler, W. (2002). *Spiking neuron models*. Cambridge University Press.
- Glackin, B., McGinnity, T., Maguire, L., Wu, Q., & Belatreche, A. (2005). A novel approach for the implementation of large scale spiking neural networks on FPGA hardware. In *Proc. IWANN 2005 computational intelligence and bioinspired systems* (pp. 552–563).
- Gurney, K. (1997). *An introduction to neural networks*. UCL Press (Taylor & Francis group).
- Hopfield, J. J. (1982). Neural networks and physical systems with emergent collective computational abilities. *Proceedings of the National Academy of Sciences of the United States of America*, 79(8), 2554–2558.
- Indiveri, G., Chicca, E., & Douglas, R. (2006). A vlsi array of low-power spiking neurons and bistable synapses with spike-timing dependent plasticity. *IEEE Transactions on Neural Networks*, 17(1), 211–221.
- Jung, R., Brauer, E., & Abbas, J. (2001). Real-time interaction between a neuromorphic electronic circuit and the spinal cord. *IEEE Transactions on Neural Systems and Rehabilitation Engineering*, 9(3), 319–326.
- Le Masson, G., Renaud-Le Masson, S., Debay, D., & Bal, T. (2002). Feedback inhibition controls spike transfer in hybrid thalamic circuits. *Nature*, 417(6891), 854–858.
- Lewis, N., & Renaud, S. (2007). Spiking neural networks “in silico”: from single neurons to large scale networks. In *Systems, signal and devices conference, 2007*.
- Likharev, K., Mayr, A., Muckra, I., & Turel, O. (2003). Crossnets—high-performance neuromorphic architectures for cmol circuits. In J. Reimers, C. Picconatto, J. Ellenbogen, & R. Shashidhar (Eds.), *Ann. NY Acad. Sci. New York Acad. Sciences: Vol. 1006. Molecular electronics III* (pp. 146–163).
- Linares-Barranco, B., Sanchez-Sinencio, E., Rodriguez-Vazquez, A., & Huertas, J. (1993). A cmos analog adaptive bam with on-chip learning and weight refreshing. *IEEE Transactions on Neural Networks*, 4(3), 445–455.
- Linares-Barranco, B., & Serrano-Gotarredona, T. (2009). Memristance can explain spike-time-dependent-plasticity in neural synapses. <http://hdl.handle.net/10101/npre.2009.3010.1>.
- Mahowald, M., & Douglas, R. (1991). A silicon neuron. *Nature*, 354(6354), 515–518.
- Minsky, M. L., & Papert, S. A. (1969). *Perceptrons*. Cambridge, MA: MIT Press.
- Munakata, T. (2008). *Fundamentals of the new artificial intelligence: neural, evolutionary, fuzzy and more* (2nd ed.). Springer.
- Pavlov, I. (1927). *Conditioned reflexes: an investigation of the physiological activity of the cerebral cortex*. London: Oxford University Press, (translated by G. V. Anrep).
- Pershin, Y. V., & Di Ventra, M. (2009a). Frequency doubling and memory effects in the spin Hall effect. *Physical Review B*, 79(15), 153307.
- Pershin, Y. V., & Di Ventra, M. (2009b). Practical approach to programmable analog circuits with memristors. *IEEE Transactions on Circuits and Systems I* (in press). arXiv:0908.3162.
- Pershin, Y. V., & Di Ventra, M. (2010). Memristive circuits simulate memcapacitors and meminductors. *Electronics Letters*, 46, 517–518.
- Pershin, Y. V., La Fontaine, S., & Di Ventra, M. (2009). Memristive model of amoeba learning. *Physical Review E*, 80, 021926.
- Pershin, Y. V., & Ventra, M. D. (2008). Spin memristive systems: spin memory effects in semiconductor spintronics. *Physical Review B*, 78, 113309.
- Rojas, R. (1996). *Neural networks—a systematic introduction*. Berlin: Springer-Verlag.
- Rosenblatt, F. (1958). The perceptron: a probabilistic model for information storage and organization in the brain. *Psychological Review*, 65(6), 386–408.
- Schemmel, J., Meier, K., & Mueller, E. (2004). A new VLSI model of neural microcircuits including spike time dependent plasticity. In *Proceedings of ESANN2004* (pp. 405–410).
- Snider, G. S. (2008). Cortical computing with memristive nanodevices. *SciDAC Review*, 10, 58–65.
- Sorensen, M., DeWeerth, S., Cymbalyuk, G., & Calabrese, R. (2004). Using a hybrid neural system to reveal regulation of neuronal network activity by an intrinsic current. *Journal of Neuroscience*, 24(23), 5427–5438.
- Strukov, D. B., Snider, G. S., Stewart, D. R., & Williams, R. S. (2008). The missing memristor found. *Nature*, 453, 80–83.
- Stuart, G., Spruston, N., Sakmann, B., & Hausser, M. (1997). Action potential initiation and backpropagation in neurons of the mammalian CNS. *Trends in Neuroscience*, 20(3), 125–131.
- Vogelstein, R., Malik, U., & Cauwenberghs, G. (2007). Silicon spikebased synaptic array and address-event transceiver. In *Proceedings of ISCAS04: Vol. 5* (pp. 385–388).
- Waters, J., Schaefer, A., & Sakmann, B. (2005). Backpropagating action potentials in neurons: measurement, mechanisms and potential functions. *Progress in Biophysics & Molecular Biology*, 87, 145–170.
- Widrow, B. (1962). Rate of adaptation of control systems. *ARS Journal*, 32(9), 1378–1385.
- Yang, J. J., Pickett, M. D., Li, X., Ohlberg, D. A. A., Stewart, D. R., & Williams, R. S. (2008). Memristive switching mechanism for metal/oxide/metal nanodevices. *Nature Nanotechnology*, 3(7), 429–433.